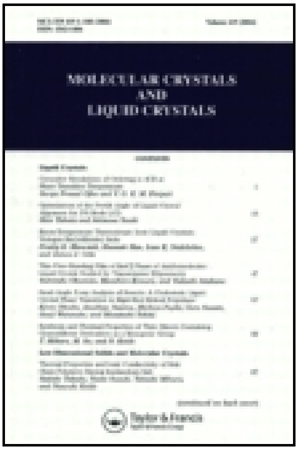

Molecular Crystals and Liquid Crystals
Publication details, including instructions for authors and subscription information:
http://www.tandfonline.com/loi/gmcl20

Fabrication of Paraelectric Nanocolloidal Liquid Crystals

Hari M. Atkuri [a], Ke Zhang [a] & John L. West [a]
[a] Liquid Crystal Institute & Department of Physics, Kent State University, Kent, OH, U.S.A.

Version of record first published: 05 Oct 2009

To cite this article: Hari M. Atkuri, Ke Zhang & John L. West (2009): Fabrication of Paraelectric Nanocolloidal Liquid Crystals, Molecular Crystals and Liquid Crystals, 508:1, 183/[545]-190/[552]

To link to this article: http://dx.doi.org/10.1080/15421400903060581

Mol. Cryst. Liq. Cryst., Vol. 508, pp. 183/[545]–190/[552], 2009
Copyright © Taylor & Francis Group, LLC
ISSN: 1542-1406 print/1563-5287 online
DOI: 10.1080/15421400903060581

Fabrication of Paraelectric Nanocolloidal Liquid Crystals

Hari M. Atkuri, Ke Zhang, and John L. West
Liquid Crystal Institute & Department of Physics, Kent State
University, Kent, OH, U.S.A.

Ferroelectric nanoparticle suspensions can enhance the properties of liquid crystals; increasing key parameters such as clearing point, birefringence and dielectric anisotropy. However, these suspensions are difficult to reliably prepare. The interaction between surfactant and ferroelectric particles plays a crucial role in determining the performance and stability of these suspensions. Here we focus on producing ferroelectric nanoparticles using a ball milling process. Using convenient Fourier Transform Infrared Spectroscopy (FTIR) we demonstrate an effective means to monitor the surfactant distribution during the milling process. We also found that the Curie transition from the ferroelectric to paraelectic state of the particles is dependent on both the milling time and surfactant concentrations.

Keywords: $BaTiO_3$; Curie transition; ferroelectricity; ferroelectric nanoparticle; FTIR; high energy ball milling; oleic acid; surface coverage

INTRODUCTION

Dispersing particles into liquid crystals (LCs) is increasingly studied as a method to enhance the properties of LCs and produce new functional materials. Anchoring of LC molecules on microparticles surface, WR (where W is anchoring coefficient, $\sim 10^{-6}$ N/m and R is the particle radius, $\sim 10^{-5}$ m), is $\sim 10^{-11}$ N and is of a similar order as the elastic constant, K. As a result, this surface anchoring induces long range orientation distortions in the LC medium which produces intriguing defects. To minimize these distortions, the particles tend to aggregate and thereby share their defects. This produces an ordered colloidal assembly [1–8]. At high concentrations, these LC colloids exhibit unique electro-optic [9,10] and viscoelastic [11,12] properties and are promising for advanced applications. As the particles size

Address correspondence to Dr. Ke Zhang, Liquid Crystal Institute and Department of Physics, Kent State University, Kent, OH 44242, USA. E-mail: kzhang@lci.kent.edu

shrinks to the nanometer scale, (10^{-7}–10^{-9} m, i.e., they are close to the size of LC molecules), $WR \ll K$, the surface anchoring induced elastic distortion is diminished. The particle's intrinsic properties therefore become more influential in determining the properties of the LC nanocolloids. A variety of nanoparticles of different nature, like ferromagnetic [13,14], metal [15,16], fullerene [17,18], carbon nanotube [19], inorganic MgO or SiO [20], and etc., have been dispersed into LCs and brings exciting features to the LC hosts.

We studied ferroelectric nanoparticles, having enormous dielectric constants in their single crystals [24]. By dispersing low concentrations of ferroelectric nanoparticles into LCs, we have developed a novel class of paraelectric nanocolloids liquid crystals (PNCLCs) which exhibit significantly enhanced dielectric, optical properties for display applications [21–23]. Because these nanopartilces produce no defects the particles are uniformly dispersed in the LC host. The new PNCLCs appear as stable and as homogenous as the pure LC. With further development they may be used in a variety of applications, replacing conventional liquid crystal formulations.

We have found that the properties of the ferroelectric particles are extremely sensitive to their preparation techniques and conditions. We are only now learning how to balance a variety of factors, like the particle's dipole moment, size, shape, and the surfactant's concentration and distribution, to achieve high quality ferroelectric particles. In our study, we utilized a conventional high energy ball milling process to obtain nano-sized ferroelectric particles used to produce the liquid crystal dispersions. Complete surfactant coverage of the particles reduces the particle aggregation and enhances the stability of suspension. More importantly, we found the surfactant layer maintains the ferroelectricity of the particles. However, excess surfactant suppresses the order parameter of the liquid crystal and wipes out the effect of the ferroelectric particles. Therefore, it is important to precisely control the surfactant concentration during the milling process in order to optimize the properties of ferroelectric liquid crystal colloids. In this paper, we introduce an FTIR technique to analyze the ratio between the free-suspended or the particle-bound surfactant molecules, and its evolution with milling time. This an important tool to establish a reproducible fabrication process for PNCLCs.

EXPERIMENTAL

At present, no suitable ferroelectric nanoparticle materials are commercially available. The commercial ferroelectric nanopowders are usually the ingredients for making ferroelectric ceramic materials.

They are pulverized from large crystal and sieved to nominal size range. Most of these particles lose their polarization due to strong mechanical collisions in this process during milling. If there is any remaining, their strong dipolar moment can induce severe agglomeration over µm scale. These powders need to be compounded with binding material and sintered at high temperature (>1000°C). Usually a high voltage (>kV) poling is required. These post treatments help to restore the polarization lost during pulverization process.

However, both these treatments are difficult to be realized in PNCLCs. For these reasons, we developed our own techniques to produce fresh ferroelectric nanoparticles in house and mixed with LC usually within hours after production to reduce the chance of aggregation, as shown in Figure 1. We selected the classic ferroelectric material, barium titanate ($BaTiO_3$) (Aldrich, ~3 µm powder), and used a planetary ball mill (Retsch, PM200) to achieve nanosized particles. The ferroelectricity of the purchased $BaTiO_3$ powder is confirmed by the Curie (ferroelectric to paraelectric) transition seen in DSC (Differential Scanning Calorimetry) measurements, as well as the characteristic hexagonal crystal structure revealed in XRD (X ray diffraction) study. Our grinding samples consisted of 1 g of $BaTiO_3$ powder, 1.5 g of oleic acid (as surfactant, 99.9%, Aldrich), 10 g heptane (act as liquid carrier, HPLC grade, Aldrich), and 100 g grinding balls (Retsch, yttrium-stabilized Zirconium oxide balls, 2 mm in diameter). These were placed into the grinding jar (Retsch, 50 ml jar with zirconium

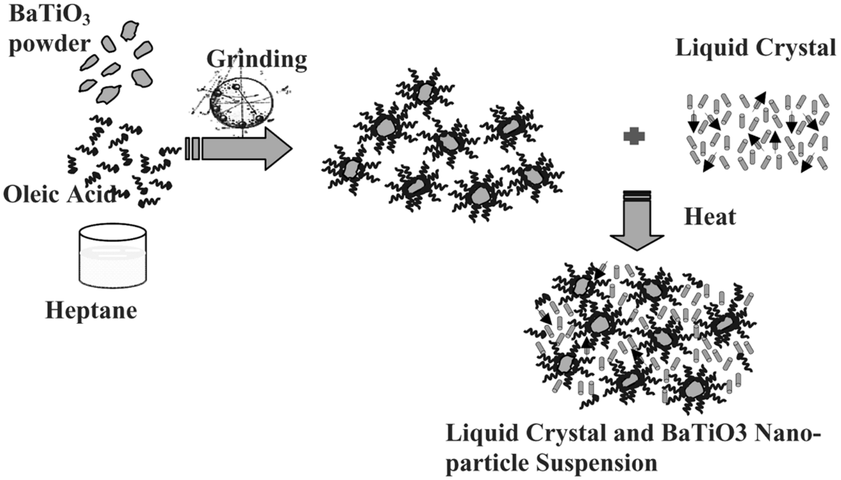

FIGURE 1 Illustration of the fabrication process of the PNCLCs.

oxide interior). The mixture was milled at 500 rpm for a designated time (5 to 60 hours). The ground particle suspension can be directly spin coated on NaCl plate for FTIR analysis of the oleic acid distribution. The ground particles were sedimented using centrifuge, and weighed after evaporation of heptane. Their ferroelectricity was assessed based on the Curie transition in the DSC measurements.

RESULTS

In earlier papers [25,26] we have proposed that the enhancement of liquid crystal properties (like phase transition temperature, dielectric anisotropy, and birefringence) may be caused by the increase of the order parameter resulting from liquid crystal molecules being aligned by the strong local electric field associated with ferroelectric nanoparticles. In order to achieve this effect, several conditions need to be met simultaneously: 1) the particles need to be large enough to possess significant dipole moment; 2) this dipole moment can be felt by the neighboring liquid crystal molecules; the particles need to be small enough to avoid the formation of defects 3) their must be enough surfactant to coat the particles 4) there must not be excess free surfactant which will reduce the order parameter.

Here we focus on how to optimize the amount of surfactant included in the mixture. The strong C=O stretch of oleic acid serves a convenient probe for quantitative FTIR analysis. We observe the absorption peak of C=O appear at $\sim 1700\,\mathrm{cm}^{-1}$, $\sim 1750\,\mathrm{cm}^{-1}$, ~ 1500–$1600\,\mathrm{cm}^{-1}$ when oleic acid presents as a dimer, monomer, or complex conjugate with $BaTiO_3$ (as shown in Figure 2), respectively [27–29]. No interference absorption can be found from heptane in $1500 \sim 1800\,\mathrm{cm}^{-1}$ range, which greatly simplified and accelerated the sample analysis.

During grinding, the particle size decreases and the total surface area increases. As a result, more oleic acid molecules bond to the particle so the $1550\,\mathrm{cm}^{-1}$ absorption (A_{1550}) increases while the $1700\,\mathrm{cm}^{-1}$ dimeric absorbance (A_{1700}) decreases. As shown in Figure 3, the ratio of the two absorbance A_{1700}/A_{1550} decreases with grinding time reaching a minimum after $\sim$15 hours of milling. This indicates that all the oleic acid molecules is bound to the $BaTiO_3$ after 15 hours. Similarly, one can also monitor the ratio of $A_{1550}/(A_{1700} + A_{1550})$ which increases with grinding and saturates after 15 hours. Because unbound (dimeric) oleic acid suppresses the liquid crystal order, it is clear one should disperse the ground particle suspension with liquid crystal at or after the saturation point.

Another important parameter we can use to monitor is the particle's ferroelectricity. It was widely agreed that below a critical size, the

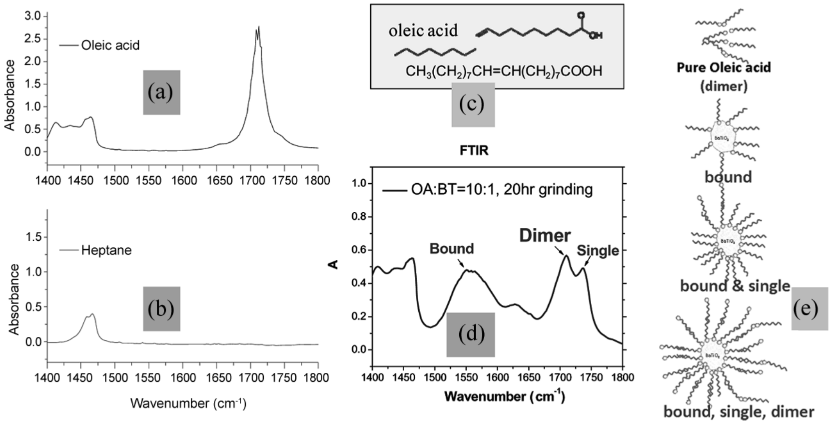

FIGURE 2 FTIR analysis of ground BaTiO3. Pure oleic acid (a) and heptane (b) shows no absorption peak in 1500 to 1650 cm^{-1} range. In pure oleic acid, strong hydrogen bonding results the formation of dimers (e), which shows C=O stretch at ~1700 cm^{-1} (d). When oleic acid forms complex conjugate with $BaTiO_3$, the C=O stretch was shifted to ~1550 cm^{-1}. A typical ground particle suspension contains three status of oleic acid molecules is shown as d.

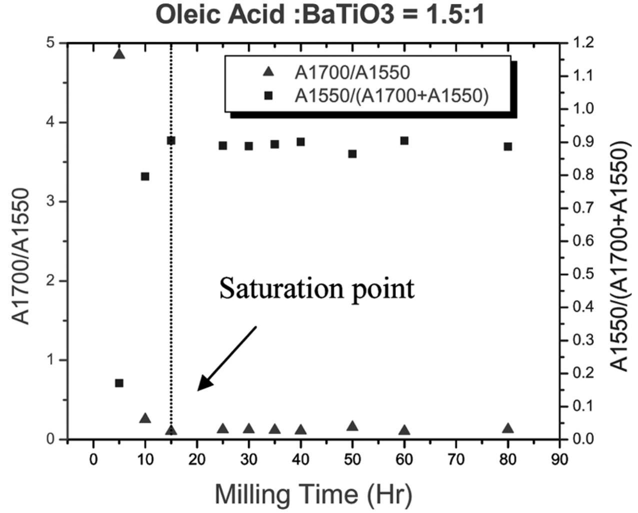

FIGURE 3 The state of oleic acid changes with milling time. The ratio of dimer vs bound oleic acid (A1700/A1550, ▲) decrease as grinding time increase and saturate at ~0 in after 15 hours of grinding. Another ratio of bound vs bound plus dimer state (A1550/[A1700 + A1550], ■) increase with grinding time and equilibrate after 15 hours of grinding.

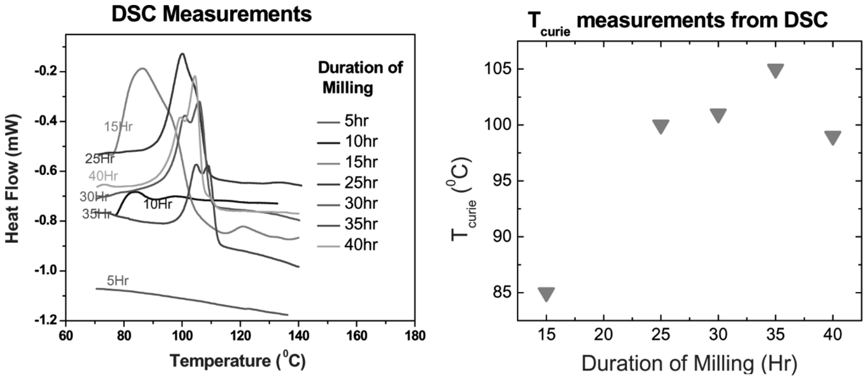

(a) (b)

FIGURE 4 DSC study of Curie transition of ground $BaTiO_3$ particles after different milling times. The ratio of oleic acid to $BaTiO_3$ here is 1.5 to 1 for all the curves. The T_{Curie} also increases with grinding time, reach a maximum at ~35 hours of grinding and decrease eventually.

particle can not been poled, even in a single domain crystal. On the other hand, we found the the Curie transition of the particles can disappear by high energy ball milling if no surfactant is present. For these reasons, we need to optimize both the milling time (to achieve small particle size and narrow size distribution) and surfactant concentration (to maintain the ferroelectricity during milling). Using DSC, we directly analyzed the Curie transition of the particles as a function of milling time. We observed, as demonstrated in Figure 4, the T_{Curie} first increases with milling, then reaches its peak value and declines after further milling. It is also clear that the Curie transition peak become more prominent and narrower as T_{Curie} is higher. It is worth noticing that the T_{Curie} peaks at ~35 hours of milling, which is different with the saturation point for oleic acid coverage shown in Figure 3. We are currently trying to optimize both T_{Curie} with oleic acid simultaneously. Also further investigations were targeted at the relationship between the particle size, spontaneous polarization and Curie transition.

SUMMARY

We demonstrated that FTIR and DSC are effective tools to analyze the properties of the ferroelectric particle suspension before dispersed into the liquid crystal host. The FTIR study shows C=O stretching band from dimeric, monomeric and conjugated oleic acid serve as a powerful probe to quickly and effectively identify and quantify the status of oleic acid. Meanwhile, DSC study demonstrate the a maximum T_{Curie}. Using both FTIR and DSC we can optimize the particle size, oleic acid concentration, and particle ferroelectricity to produce the maximum effect defined by the point where the oleic acid just enough to cover the entire particle surface and protect ferroelectricity.

REFERENCES

[1] Kuksenok, O. V., Ruhwandl, R. W., Shiyanovskii, S. V., & Terentjev, E. M. (1996). Director structure around a colloid particle suspended in a nematic liquid crystal. *Phys. Rev. E*, *54*, 5198–5203.

[2] Lubensky, T. C., Pettey, D., & Currier, N. (1998). Topological defects and interactions in nematic emulsions. *Phys. Rev. E*, *57*, 610–625.

[3] Poulin, P. & Weitz, D. A. (1998). Inverted and multiple nematic emulsions. *Phys. Rev. E*, *57*, 626–637.

[4] Stark, H. (1999). Director field configurations around a spherical particle in a nematic liquid crystal. *Eur. Phys. J. B*, *10*, 311–321.

[5] Ruhwandl, R. W. & Terentjev, E. M. (1997). Long-range forces and aggregation of colloid particles in a nematic liquid crystal. *Phys. Rev. E*, *55*, 2958–2961.

[6] Poulin, P., Stark, H., Lubensky, T. C., & Weitz, D. A. (1997). Novel colloidal interactions in anisotropic fluids. *Science*, *275*, 1770–1773.

[7] Lev, B. I. & Tomchuk, P. M. (1999). Interaction of foreign macrodroplets in a nematic liquid crystal and induced supermolecular structures. *Phys. Rev. E*, *59*, 591–602.

[8] Loudet, J. C., Barois, P., & Poulin, P. (2000). Colloidal ordering from phase separation in a liquid-crystalline continuous phase. *Nature*, *407*, 611–613.

[9] Nakamura, H., Meeker, S. P., Taira, Y., Poon, W. C. K. & Crain, J. (2001). Optical properties of colloid liquid crystal composites. *Mol. Cryst. Liq. Cryst.*, *368*, 167–174.

[10] Aliev, F. M., Kreuzer, M., & Panarin, Y. P. (1999). The dynamic properties of 5CB filled with aerosil particles investigated by PCS. *Mat. Res. Soc. Symp. Proc.*, *559*, 223–228.

[11] Boxtel, M. C. W. V., Janssen, R. H. C., Bastiaansen, C. W. M., & Broer, D. J. (2001). Viscoelastic liquid crystal colloids for the continuous processing of twist nematic electro-optical cells. *J. Appl. Phys.*, *89*, 838–842.

[12] Anderson, V. J. & Terentjev, E. M. (2001). Cellular solid behaviour of liquid crystal colloids 2. Mechanical properties. *Eur. Phys. J. E*, *4*, 21–28.

[13] Brochard, F. & de Gennes, P.G. (1970). Theory of magnetic suspensions in liquid crystals. *J. Phys. (Paris)*, *31*, 691–708.

[14] Chen, S. H. & Amer, N. M. (1983). Observation of macroscopic collective behavior and new texture in magnetically doped liquid crystals. *Phys. Rev. Lett.*, *51*, 2298–2301.

[15] Kaur, S., Singh, S. P., Biradar, A. M., Choudhary, A., & Sreenivas, K. (2007). Enhanced electro-optical properties in gold nanoparticles doped ferroelectric liquid crystals. *Appl. Phys. Lett.*, *91*, 023120/1–023120/3.

[16] Shiraishi, Y., Toshima, N., Maeda, K., Yoshikawa, H., Xu, J., & Kobayashi, S. (2002). Frequency modulation response of a liquid-crystal electro-optic device doped with nanoparticles. *Appl. Phys. Lett.*, *81*, 2845–2847.

[17] Suzuki, M., Furue, H., & Kobayashi, S. (2001). Polarizerless nanomaterial doped guest-host LCD exhibiting high luminance and good legibility. *Mol. Cryst. Liq. Cryst.*, *368*, 191–196.

[18] Khoo, I. C. (1995). Holographic grating formation in dye- and fullerene C60-doped nematic liquid-crystal film. *Opt. Lett.*, *20*, 2137–2139.

[19] Chen, H., Lee, W., & Clark, N. A. (2007). Faster electro-optical response characteristics of a carbon – nanotube nematic suspension. *Appl. Phys. Lett.*, *90*, 033510/1–033510/3.

[20] Haraguchi, F., Inoue, K., Toshima, N., Kobayashi, S., & Takatoh, K. (2007). Reduction of the threshold voltages of nematic liquid crystal electrooptical devices by doping inorganic nanoparticles. *Jpn. J. Appl. Phys.*, *46*, L796–L797.

[21] Buluy, O., Ouskova, E., Reznikov, Yu., & Litvin, P. (2004). Preparation and properties of a ferromagnetic nematic suspension. *Ukrains'kii Fizichnii Zhurnal*, *49*, A48–A50.

[22] Reznikov, Yu., Buchnev, O., Tereshchenko, O., Reshetnyak, V., Glushchenko, A., & West, J. (2003). Ferroelectric Nematic Suspension. *Appl. Phys. Lett.*, *82*, 1917–1919.

[23] Cheon, C. I., Li, L., Glushchenko, A., West, J. L., Reznikov, Yu., Kim, J. S., & Kim, D. H. (2005). Electro-optics of liquid crystals doped with ferroelectric nano-powder. *SID Symp. Digest Tech Papers*, *36*, 1471–1473.

[24] Lines, M. E. & Glass, A. M. (1977). *Principles and applications of ferroelectrics and related materials*, Clarendon Press: Oxford.

[25] Li, F., Buchnev, O., Cheon, C. I., Glushchenko, A., Reshetnyak, V., Reznikov, Y., Sluckin, T. J., & West, J. L. (2006). Orientational Coupling Amplification in Ferroelectric Nematic Colloids. *Phys. Rev. Lett.*, *97*, 147801/1–147801/4.

[26] Li, F., Buchnev, O., Cheon, C. I., Glushchenko, A., Reshetnyak, V., Reznikov, Y., Sluckin, T. J., & West, J. L. (2007). Erratum: Orientational Coupling Amplification in Ferroelectric Nematic Colloids. *Phys. Rev. Lett.*, *99*, 219901.

[27] Lee, D. H., Condrate, R. A., Sr.. (1999). FTIR spectral characterization of thin film coatings of oleic acid on glasses: I. Coatings on glasses from ethyl alcohol. *J. Mater. Sci.*, *34*, 139–146.

[28] Lee, D. H., Condrate, R. A., Sr., & Lacourse, W. C. (2000). FTIR spectral characterization of thin film coatings of oleic acid on glasses Part II Coatings on glass from different media such as water, alcohol, benzene and air. *J. Mater. Sci.*, *35*, 4961–4970.

[29] Zhang, L., He, R., & Gu, H.-C. (2006). Oleic acid coating on the monodisperse magnetite nanoparticles. *Appl. Surf. Sci.*, *253*, 2611–2617.